A Structural Basis for Neuropathic Pain Syndromes Associated with Mutations in $Na_v1.7$

Natasha Marie Powell

A thesis submitted in partial fulfillment of the degree

requirements for the degree of

Master of Science

University of Washington

2020

Committee:

William N Zagotta

William A Catterall

Sharona Gordon

Charles Asbury

Program Authorized to Offer Degree:

Neuroscience

University of Washington

Abstract

A Structural Basis for Neuropathic Pain Syndromes Associated with Mutations in $Na_v1.7$

Natasha Marie Powell

Chair of the Supervisory Committee:

William N Zagotta

Department of Physiology and Biophysics

Voltage-gated sodium channels (Na_vs) are responsible for the upstroke of action potentials in electrically excitable cells. Transmission of nociceptive information from the body periphery to the central nervous system is mediated by specific isoforms of Na_vs present in dorsal root ganglion (DRG) and trigeminal ganglion (TG) sensory neurons. $Na_v1.7$ is the most abundantly expressed isoform in DRG and TG neurons, and an isoleucine to valine mutation at residue 136 in the voltage-sensing domain (VSD) results in the disease, inherited erythromelalgia (IEM). From functional studies, it is clear that mutation at this residue results in increased $Na_v1.7$ excitability, though the source of this hyperexcitability remains to be discovered. Here, we introduced a homologous isoleucine to valine mutation (residue 22) in the ancestral bacterial channel, Na_vAb, and present a X-ray crystallography structure of the mutant channel. Small shifts in the entire S1 segment and decreased interaction between residue 22 and charged arginine residues in the VSD were observed. This data supports a structural basis for the hyperexcitability of $Na_v1.7$ associated with the IEM-causing mutation at residue 136.

Table of Contents

I. Introduction……...…… p. 5

II. Methods……..p. 9

III. Results……..……..p. 11

IV. Discussion……..…….p. 12

V. Proposal for Future Work…..…….…….……..p. 14

Acknowledgements

I would like to thank Dr. Bill Catterall and the entire Catterall Lab for their support, especially Dr. George Wisedchaisri and Dr. Eedann McCord for their technical support. I would also like to thank Dr. Sharona Gordon and Dr. Bill Zagotta for their endless moral support and encouragement throughout an exceptionally difficult period of my life. Finally, thank you to my graduate school cohort – Asad Beck, Emily Brown, Kristen Drummy, Nastacia Goodwin, Lila Levinson, German Rojas, and Sierra Schelufer – for being the best friends I could ever ask for and for standing by me. This research was supported by the Graduate Program in Neuroscience, a National Research Service award from Training Grant T32, and a National Institutes of Health Research Grant R01 NS15751 to William A Catterall.

Dedication

This work is dedicated to several individuals: Dr. John Ohlfest, Dr. Adam Littermann, and Dave Zellmer, the three individuals who gave me my first introduction to scientific research and ultimately motivated me to pursue a graduate degree; Dr. Thomas Cech, who taught me how to think critically and inspired me to study biochemistry; Dr. Sumit Borah, who taught me how to conduct rigorous experiments and encouraged me to never give up; my Mom, who has been there for me through all the good times, and tough ones too; and to my Grandma and Grandpa, who believed I could touch the stars if I just jumped high enough.

I. INTRODUCTION

Neuropathic pain is defined by the International Association for the Study of Pain as "pain caused by lesion or disease of the somatosensory nervous system." Approximately 7-18% of individuals experience peripheral neuropathic pain to varying degrees (Laedermann et al., 2015). Drugs currently available are not sufficient to treat these individuals, since they manage symptoms of neuropathic pain rather than treating its underlying cause. Following injury, there are observable increases in voltage-gated sodium channel (Na_v) expression that correlate with spontaneous activity of sensory neuron afferents. Hyperexcitability of these neurons is responsible for lasting sensitization in the somatosensory system (Laedermann et al., 2015; Yang et al., 2008).

Na_vs are essential to the propagation of action potentials as they are responsible for the upstroke of the action potential. Transmission of nociceptive information from the periphery to the central nervous system is mediated by specific isoforms of Na_vs present in dorsal root ganglion (DRG) and trigeminal ganglion (TG) sensory neurons. DRG and TG sensory neurons contain the majority of nine biophysically distinct isoforms of Na_vs, though the isoforms $Na_v1.7$, $Na_v1.8$, and $Na_v1.9$ are the most abundantly expressed. Of these, $Na_v1.7$ is the most abundantly expressed and plays an essential role in modulating the perception of pain (Yang et al., 2008). Mutations in the gene encoding $Na_v1.7$, *SCN9A*, are associated with severe episodic hypersensitivity to pain as well as congenital insensitivity to pain (Laedermann et al., 2015).

1.1. Structure and Function of Sodium Channels

Sodium channels (Na_vs) were first biochemically characterized in 1980 (Beneski and Catterall, 1980) and since, enormous effort has been made to understand their structure and function. Na_vs consist of alpha and beta subunits in an assumed stoichiometry of 1:1 (Catterall, 1992). The alpha-subunit is encoded by a single gene, which is structurally divided into four homologous domains

(I-IV) while four different genes encode different beta-subunits. Each domain of the alpha-subunit is connected to another via an intracellular loop, forming a heterotetramer of ~330kDa, and each domain contains six alpha-helical transmembrane segments (S1-S6). S5 and S6 constitute the channel pore while S1-S4 act as sensors of voltage changes. Nine discrete genes (*SCNxA*) encode for the alpha-subunits: isoforms $Na_v1.1$ to $Na_v1.9$ and the atypical tenth isoform, NaX (Akopian et al., 1997; Noda and Hiyama, 2014). Each isoform has distinct biophysical properties and distinct expression patterns throughout the nervous system.

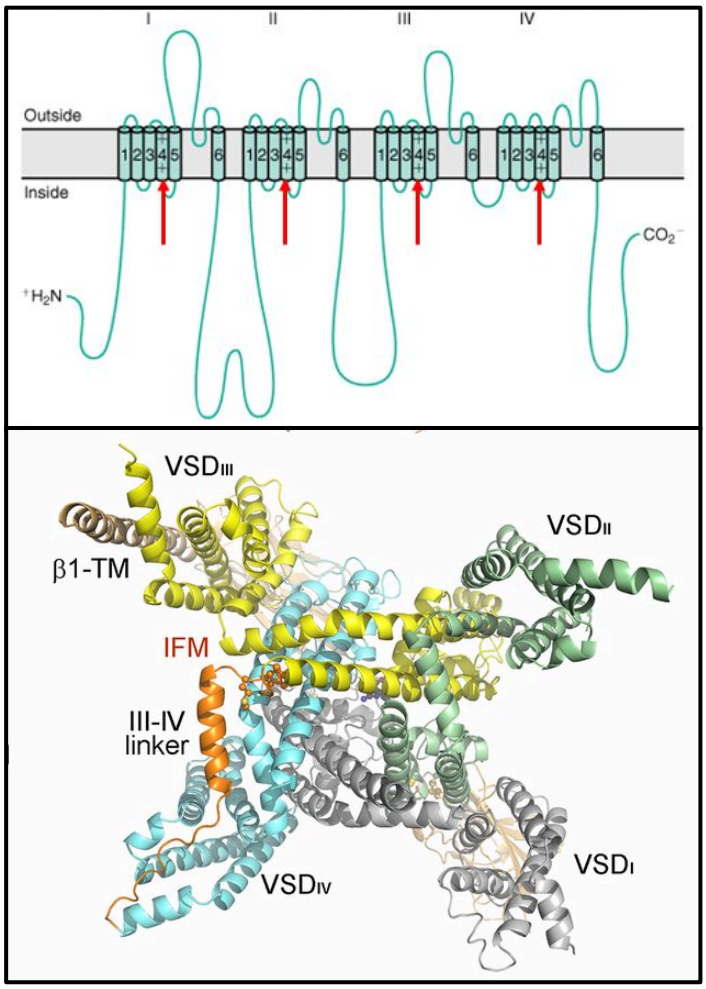

Figure 1 Structure of typical sodium channels shown in diagram form (top panel) and in ribbon diagram (lower panel).

The pore-forming alpha-subunit enables sodium conductance, while the beta-subunits modulate the biophysical properties and membrane stabilization of Na_vs (Isom et al., 1995). Eukaryotic Na_vs contain four voltage-sensor domains (VSD1-4) that surround a central pore module in a domain-swapped arrangement (Pan et al., 2018). VSDs are helical bundles (S1-S4) that respond to changes in membrane potential by virtue of positively charged arginine residues conserved along the S4 helix in an RxxR motif (Bezanilla, 2018). These arginine gating charges move across a narrow hydrophobic constriction within the VSDs

facilitated by interactions with acidic and polar residues from neighboring S1-S3 segments (Groome and Winston, 2013; Pless et al., 2014).

When membrane depolarization occurs, outward movement of the S4 gating charges couples through the intracellular S4-S5 linkers to widen the S6 helical bundle crossing, initiating ion conductance (Muroi et al., 2010). Rapid VSD1-3 activation is necessary to open the S6 gate, while VSD4 activation initiates a fast inactivation process (Capes et al., 2013). In the resting state, the S4 segment of the VSD is drawn intracellularly. Three gating charges pass through the membrane electric field and this movement forms an elbow which connects S4 to the S4-S5 linker and tightens the S6 helical bundle crossing to prevent channel opening (Wisedchaisri et al., 2019). Recent high-resolution cryoEM structures of a single sodium channel support the classical "sliding helix" mechanism of voltage sensing that describes a complete gating mechanism for voltage sensor function, pore opening, and activation-gate closure (Wisedchaisri et al., 2019).

1.2 Na_v Isoforms Expressed in Nociceptive Neurons and their Implication in Pain Syndromes

With the exception of two isoforms ($Na_v1.2$ and $Na_v1.4$), all Na_v isoforms are expressed in nociceptive neurons and collaborate for electrogenesis (Black et al., 1996; Rush et al., 2007; Berta et al., 2008; Fukuoka and Noguchi, 2011; Ho and O'Leary, 2011). Of these isoforms, $Na_v1.7$, $Na_v1.8$, and $Na_v1.9$ are the most abundantly expressed among dorsal root ganglion (DRG) neurons (Black et al., 1996; Toledo-Aral., 1997; Berta et al., 2008; Ho and O'Leary, 2011; Dib-Hajj et al. 2013). Throughout the last decade, mutations in $Na_v1.7$, $Na_v1.8$, and $Na_v1.9$ have been linked to human pain disorders. This study has focused on $Na_v1.7$.

Familial and *de novo* mutations in $Na_v1.7$ are associated both with hypersensitivity to pain and congenital insensitivity to pain. A gain-of-function mutation in $Na_v1.7$ leads to painful inherited

channelopathies such as erythromelalgia (Cummins et al., 2004; Yang et al., 2004). Alternatively, loss-of-function mutations in $Na_v1.7$ are linked to congenital insensitivity to pain.

A point mutation at residue 136 in $Na_v1.7$ generates an isoleucine to valine swap. This mutation has been linked to inherited erythromelalgia (IEM). Patients with IEM experience severe and debilitating burning sensations in their limbs. Functional studies have revealed that this painful sensation is a result of increased $Na_v1.7$ excitability: the channel is hyperexcitable at a less positive membrane potential. The source of this hyperexcitability remains elusive. However, examining the structure of $Na_v1.7$ reveals that residue 136 is positioned such that it may interact with charged arginine residues in the VSD. Residue 136 and the fourth arginine (R4) of the VSD are within 3.3A of one another, well within the distance van der Waals interactions may be expected to occur (Figure 4). This observation led to the hypothesis that the isoleucine to valine mutation which results in the loss of a methyl group on the side chain at position 136 alters the manner in which residue 136 interacts with charged arginine residues of the VSD of $Na_v1.7$. Subsequently, the VSD may move more easily, allowing the channel to activate at more negative potentials.

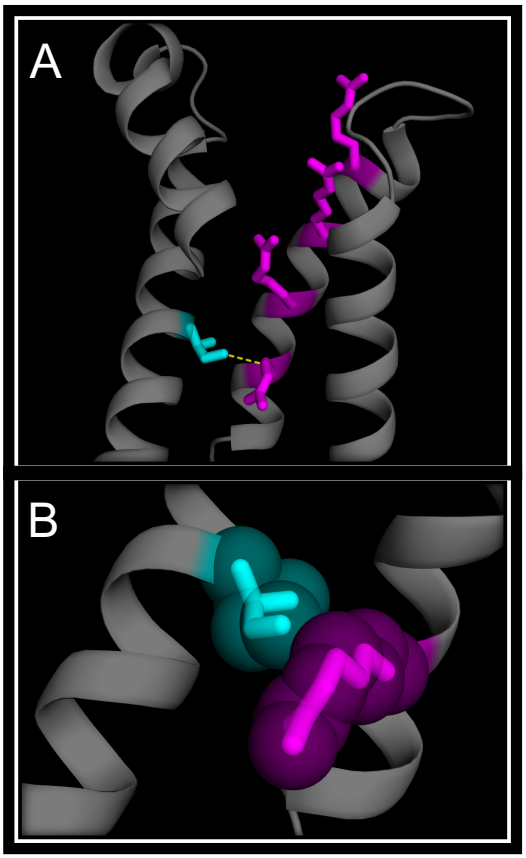

Figure 2 Residue 136 may interact with arginine rich VSD. (A) Isoleucine (cyan) in position 136 is within distance expected for van der Waals interaction with R4 (magenta) of the VSD. (B) Alternative view of position 136/R4 interaction.

All biochemical experiments were performed using Na_vAb, a sodium channel from the bacterium *Arcobacter butzleri*. As their evolutionary ancestor, Na_vAb is nearly identical in

structure and sequence to mammalian Na_vs and has the benefit of being a single domain homotetramer of ~33kDa versus mammalian channels whose size and complexity make biochemical experiments more technically challenging.

II. METHODS

2.1 Na_vAb I22V D28 ($Na_v1.7$ I136V) Construct

An isoleucine to valine mutation was introduced to Na_vAb at the residue homologous to residue 136 in Na_v1.7. The Na_vAb construct used hosts a 28 residue C-terminal truncation, as our lab has found this construct to be the best for crystallization. Throughout this thesis, the IEM mutant Na_vAb construct will be referred to as Na_vAb I22V D28.

```
                          10         20         30         40         50
NavAb   -------MYLRITNIVESSFFTKFIIYLIVLNGITMGLETSKTFMQSFGVYTTLFNQIVI
Nav1.7  IPRPGNKIQGCIFDLVTNQAFDISIMVLICLNMVTMMVEKEGQS-QHMTEVLYWINVVFI
                     120        130        140        150
```

2.2 Cell Lines

Sf9 (*Spodoptera frugiperda*) and Hi5 (*Trichoplusia ni*) insect cells were maintained and infected in Grace's Insect Medium supplemented with 7.5% FBS and glutamine/penicillin/streptomycin at 27^{o}C for baculovirus production and protein expression, respectively.

2.3 Expression and Purification of Na_vAb I22V D28 ($Na_v1.7$/I136V)

FLAG- Na_vAb D28 constructs were previously generated in the lab for structural study by X-ray crystallography. This construct was cloned into pFastBacDual vector (Life Technologies). Baculovirus harboring the construct was prepared using the Bac-to-Bac protocol. Hi5 cells were infected with P3 virus and incubated for 72-96 hours at 27°C for maximum expression. Cells were harvested by centrifugation. Cell pellets were resuspended (20mL per plate) in Buffer B, lysed by sonication, and membranes were solubilized. The mixture was centrifuged at 15,000xg for 25min

at 4°C, and the supernatant was incubated with FLAG resin for 1h at 4°C with gentle mixing. The resins were washed with Buffer C and bound protein was eluted with Buffer C supplemented with 20mg FLAG peptide. Eluted protein was concentrated to 1mL using Vivaspin20 100kDa MWCO and further purified with Superose 6 Increase size-exclusion chromatography using 10mM Tris HCl pH 7.5, 100mM NaCl, and 0.12% digitonin as a column running buffer. Elution fractions were evaluated using SDS-PAGE and peak fractions were combined and concentrated using Vivaspin6 100kDa MWCO to a final concentration of ~20mg/mL.

2.5 Crystallization Conditions

Na_vAb-bicelle complexes were prepared by mixing Na_vAb I22V D28 with 10% bicelle (7.5% w/v DMPC and 2.5% w/v CHAPSO) at 1:5 volume ratio and screened for crystallization conditions. Best crystals appeared under 1.6-1.7 M ammonium sulfate and 0.1 M sodium citrate, pH 4.6-5.2 for Na_vAb I22V D28 (Figure 3). Crystals were cryo-protected by stepwise transfers to a series of cryo-protectant solutions containing 6%–30% glucose with the same concentration of ammonium sulfate and sodium citrate pH 5.0 for Na_vAb I22V D28.

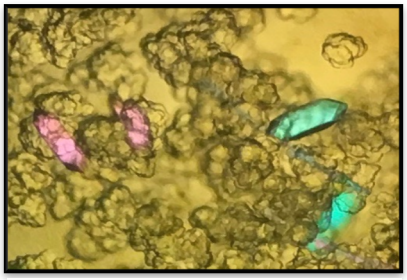

Figure 3 Sample of NavAb I22V D28 crystals harvested for X-ray crystallography

2.6 X-ray diffraction data collection and structural determination

Crystals were tested for diffraction and data were collected at Advanced Light Source (ALS) beamline 8.2.1 and 8.2.2 (HHMI). Diffraction data were processed using HKL2000 software (Otwinowski and Minor, 1997) and structures were determined by molecular replacement using PHASER (McCoy et al., 2007) and refined using REFMAC (Murshudov et al., 2011) in CCP4 program suite (Winn et al., 2011). Manual model building and local real space refinement was carried out in COOT (Emsley et al., 2010), followed by structure refinement in REFMAC.

III. RESULTS

3.1 Na_vAb I22V D28 was successfully purified for crystallization via size-exclusion chromatography

Na_vAb I22V D28 protein was purified using size-exclusion chromatography. Over 450mAU of protein was purified (peak highlighted in light blue; Figure 4A); greater than 300mAU is considered a large yield. Elution fractions from the size-exclusion were run on SDS-PAGE to verify that the protein purified was the expected molecular weight. All fractions contained protein that migrated at the expected molecular weight of ~33kDa for Na_vAb. Fractions 6-10 were combined and used for crystallization, as these fractions contained the majority of protein. Crystals appeared under 1.6-1.7 M ammonium sulfate and 0.1 M sodium citrate, pH 4.6-5.2.

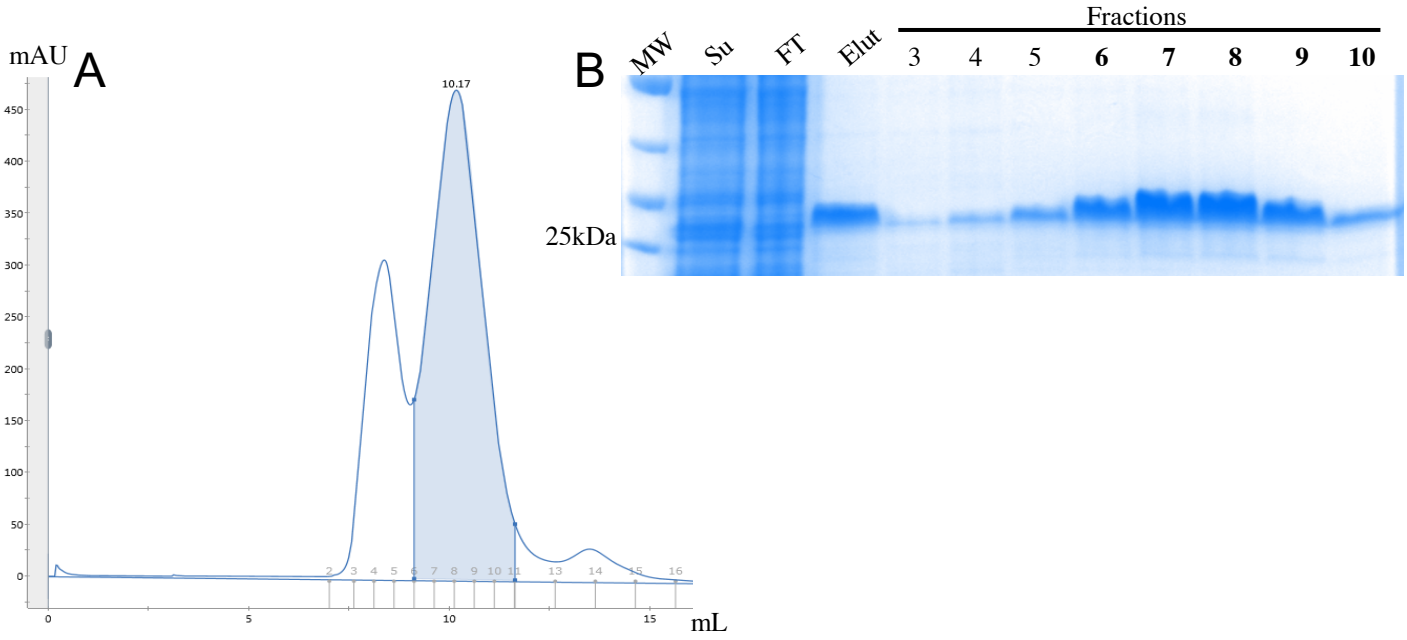

Figure 4 (A) Size-exclusion chromatography profile of protein purification of Superdex 200 column for NavAb I22V D28. The protein was expressed and purified as previously reported (Payandeh et al., 2011). (B) SDS-PAGE of peak fractions of NavAb I22V D28. Peak fractions used for protein crystallization indicated in bold. NavAb bands migrated at the expected molecular weight.

3.2 Isoleucine to valine mutation generates a small shift in the position of residue 22 and of arginines in the VSD

Diffraction data were processed as previously described (see Methods). After structure refinement to 2.7A (overall molecule), the distance between the isoleucine native to position 22 and the fourth arginine (R4) in the VSD of the S1 segment measures 3.3A when measured from the alpha carbon of the isoleucine to the alpha carbon of R4 (Figure 5A). This distance increases to 4A when residue 22 is mutated to valine, as occurs in IEM (Figure 5B). A small shift (>1A) of the entire S1 segment of Na_vAb I22V D28 relative to WT Na_vAb was observed, as well as a rotation of the R4 side chain (Figure 5C).

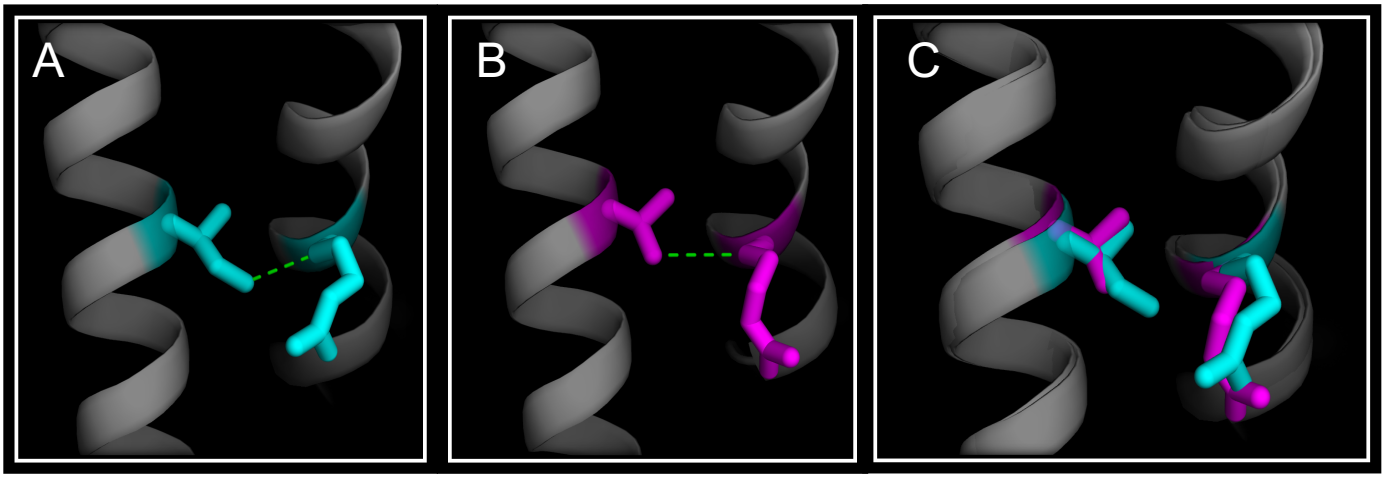

Figure 5 (A) WT Na_vAb. Native isoleucine side chain (left) 3.3A from R4 of S1 (right). (B) Na_vAb I22V D28. Mutant valine side chain (left) 4A from R4 of S1 (right). (C) Superimposition of WT Na_vAb (cyan) with Na_vAb I22V D28 (magenta).

IV. DISCUSSION

When structures of WT Na_vAb and Na_vAb I22V D28 are superimposed, it is clear that the isoleucine to valine mutation at position 22 generates a shift in the residues of the S1 VSD, as well as the entire S1 segment (Figure 5C). The shift in residues combined with the fact that the valine side chain is smaller than that of isoleucine means that R4 has more space, thereby potentially

making it easier for the VSD to move regardless of the state of the channel. If this is true, this could be the structural basis underlying the channel's ability to activate at more negative potentials in IEM.

To correlate the structural changes we observed with a functional effect, we conducted preliminary electrophysiology experiments. Unfortunately, no significant difference between WT Na_vAb and Na_vAb I22V D28 was detected. Further investigation will be required to determine the functional effect of the structural changes observed in the mutant channel.

Several mutations in $Na_v1.7$ are correlated with pain syndromes. One helical turn above the isoleucine to valine mutation that occurs at position 136 (position 22 in Na_vAb) is another position that is frequently mutated from an isoleucine to valine residue (position 739 in $Na_v1.7$; position 18 in Na_vAb). Mutation at this position results in small fiber neuropathy (SFN). We were also interested in a structural basis for this disease, so a separate construct, Na_vAb I18V D28, was interrogated alongside Na_vAb I22V D28 using the exact methods described above. Unfortunately, when the structure of Na_vAb I18V D28 was determined, no significant shifts from WT Na_vAb were observed.

If a structural basis for IEM and/or SFN were determined, that structural basis may be influential in informing drug design to lessen or eliminate the symptoms of these diseases in patients. Since both mutations occur on the intracellular side of the channel, drug design may be more challenging, though possible so long as the overall molecule is at least partially uncharged at physiological pH to cross the cellular membrane.

V. PROPOSAL FOR FUTURE WORK

Pain sensation (nociception) is a fundamental sensory mechanism but its basic mechanisms and regulation are incompletely understood. There is considerable evidence that voltage-gated sodium channels (Na_vs) in dorsal root ganglion (DRG) and trigeminal ganglion (TG) sensory neurons are dysregulated in neuropathic pain syndromes. Na_v regulation and subsequent control of sensory neuron excitability are central to the control of nociception and to preventing the development of chronic pain syndromes. However, the regulation of Na_vs in neuropathic pain syndromes is incompletely understood, and further investigation into the understanding the mechanism underlying nociceptive physiology at the atomic level must be prioritized.

Posttranslational modification (PTM) of Na_vs influences their expression level at the neuronal membrane (Laedermann et al., 2015). Ubiquitylation is a vital process controlling the internalization and degradation of Na_vs. The final, limiting step of ubiquitylation is the covalent attachment of ubiquitin molecules to lysine residues of the target channel. Ubiquitin attachment is achieved through ubiquitin protein ligase activity. One such ubiquitin ligase is Nedd4-2 (neuronal precursor cell expressed developmentally downregulated-4 type 2). This ligase is a member of the E3 subfamily whose type I WW domain interacts with PY motifs (PPxY) of target proteins. Importantly, all Na_vs expressed in DRG and TG sensory neurons contain PY motifs (Laedermann et al., 2013). To date, the exact role and relevance of Nedd4-2 in sensory neurons, as well as its implication in modulating pain sensitivity, remains to be investigated.

One may conceive a model of neuropathic pain in which decreases in Nedd4-2 expression permit increased surface expression of $Na_v1.7$. The ability to modulate the interaction between Nedd4-2 and $Na_v1.7$ could control Na_v levels in sensory neurons and, subsequently,

may control neuropathic pain perception. A structural basis for Nedd4-2, $Na_v1.7$ interactions will provide fundamental new insight at the atomic level to this crucial nociceptive process.

5.1 Specific Nedd4-2 / $Na_v1.7$ interaction

Molecular biology and biochemistry techniques could be employed to investigate the specific location at which Nedd4-2 interacts with $Na_v1.7$. Preliminary bioinformatic analyses have revealed a putative interaction site, a PY motif, for Nedd4-2 within $Na_v1.7$. Specifically, this PY motif is located near the very C-terminus of the channel's intracellular tail. The motif appears to be conserved across seven of the nine Na_v isoforms; as Na_vs are highly evolutionarily conserved (~70% protein sequence alignment) this is not surprising. $Na_v1.6$, a separate isoform expressed at lower levels than $Na_v1.7$ in DRG and TG sensory neurons, contains a similar PY motif in its C-terminal tail and has been shown to interact with Nedd4-2 via this motif, supporting the hypothesis that $Na_v1.7$ is regulated by Nedd4-2 (Laedermann et al., 2013). Pulldown assays could demonstrate an interaction between $Na_v1.7$ and Nedd4-2. Several constructs including GST fusion proteins with varying lengths of the relevant region of $Na_v1.7$ (GST- $Na_v1.7$/C-term) could be utilized in these assays. A relatively short C-terminal fusion may be sufficient to demonstrate the interaction of the two proteins, whereas longer constructs may be more appropriate for future structural experiments.

5.2 Structural analysis of $Na_v1.7$ in complex with Nedd4-2

How the structure of $Na_v1.7$ is altered with Nedd4-2 interaction is of greatest interest since this information will define the molecular mechanisms of this regulation. One may consider using X-ray crystallography to determine the initial structure of the Nedd4-2 / $Na_v1.7$ interaction. Mammalian Na_vs are large heterotetramers of around 220kDa, and attempts to crystallize the full-length channel, to date, have been unsuccessful. Therefore, a chimera of the

C-terminal region of $Na_v1.7$ with Na_vAb, a bacterial sodium channel (from *Arcobacter butzleri)*. Na_vAb shares a similar pharmacological profile, structure, and sequence with mammalian channels, may be most appropriate (Catterall et al., 2015). Na_vAb has the advantage of being a much smaller (~30kDa) homotetramer that makes performing biochemical experiments simpler. The chimera in complex with Nedd4-2 may be used to solve the structure of the protein complex by X-ray crystallography and cryo electron microscopy (cryoEM) methods. Similar methods may be applied to the entire intact $Na_v1.7$ channel via cryoEM. Although the $Na_v1.7$ structure has recently been determined by cryoEM, the C-terminal domain was not observed in the structure (Shen et al., 2019). New methods will be required to study this channel in its intact form.

REFERENCES

Akopian AN, Souslova V, Sivilotti L, Wood JN. Structure and distribution of a broadly expressed atypical sodium channel. *FEBS Lett*. **400**(2): 183-187 (1997).

Beneski DA, Catterall WA. Covalent labeling of protein components of the sodium channel with a photoactivable derivative of scorpion toxin. *Proc Natl Acad Sci U S A*. **77**(1): 639-643 (1980).

Berta T, Poirot O, Pertin M, Ji RR, Kellenberger S, Decosterd I. Transcriptional and functional profiles of voltage-gated Na^+ channels in injured and non-injured DRG neurons in the SNI model of neuropathic pain. *Mol Cell Neurosci*. **37**(2): 196-208 (2008).

Bezanilla F. Gating currents. *J Gen Physiol*. **150**(7): 911-932 (2018).

Black JA, Waxman SG. Sodium channel expression: a dynamic process in neurons and non-neuronal cells. *Dev Neurosci*. **18**(3): 139-152 (1996).

Capes DL, Goldschen-Ohm MP, Arcisio-Miranda M, Bezanilla F, Chanda B. Domain IV voltage-sensor movement is both sufficient and rate limiting for fast inactivation in sodium channels. *J Gen Physiol*. **142**(2): 101-112 (2013).

Catterall WA. Cellular and molecular biology of voltage-gated sodium channels. *Physiol Rev*. **72**(4 Suppl): S15-S48 (1992).

Catterall WA, Zheng N. Deciphering voltage-gated Na^+ and Ca^{2+} channels by studying prokaryotic ancestors. *Trends Biochem Sci.* **40**(9): 526-34 (2015).

Cummins TR, Dib-Hajj SD, Waxman SG. Electrophysiological properties of mutant Nav1.7 sodium channels in a painful inherited neuropathy. *J Neurosci*. **24**(38): 8232-8236 (2004).

Dib-Hajj SD, Yang Y, Black JA, Waxman SG. The $Na_V1.7$ sodium channel: from molecule to man. *Nat Rev Neurosci*. **14**(1): 49-62 (2013).

Emsley, P., Lohkamp, B., Scott, W.G., and Cowtan, K. Features and development of Coot. *Acta Crystallogr. D Biol. Crystallogr.* **66**: 486–501 (2010).

Fukuoka T, Noguchi K. Comparative study of voltage-gated sodium channel α-subunits in non-overlapping four neuronal populations in the rat dorsal root ganglion. *Neurosci Res*. **70**(2): 164-171 (2011).

Groome JR, Winston V. S1-S3 counter charges in the voltage sensor module of a mammalian sodium channel regulate fast inactivation [published correction appears in J Gen Physiol. 2015 Dec;**146**(6): 541-546]. *J Gen Physiol*. **141**(5): 601-618 (2013).

Guo, J., Zeng, W., Chen, Q., Lee, C., Chen, L., Yang, Y., Cang, C., Ren, D., and Jiang, Y. Structure of the voltage-gated two-pore channel TPC1 from Arabidopsis thaliana. *Nature.* **531**: 196-201 (2016).

Ho C, O'Leary ME. Single-cell analysis of sodium channel expression in dorsal root ganglion neurons. *Mol Cell Neurosci*. **46**(1): 159-166 (2011).

Isom LL, Ragsdale DS, De Jongh KS, et al. Structure and function of the beta 2 subunit of brain sodium channels, a transmembrane glycoprotein with a CAM motif. *Cell*. **83**(3): 433-442 (1995).

Kintzer, A.F., and Stroud, R.M. Structure, inhibition and regulation of two-pore channel TPC1 from Arabidopsis thaliana. *Nature.* **531**: 258–262 (2016).

Laedermann, CJ *et al*. Dysregulation of voltage-gated sodium channels by ubiquitin ligase NEDD4-2 in neuropathic pain. *J Clin Invset.* **123**(3): 3002-3013 (2013).

Laedermann CJ, Abriel, H, Decosterd I. Post-translational modifications of voltage-gated sodium channels in chronic pain syndromes. *Front Pharmacol.* **6**:263 (2015).

Li, Q., Wanderling, S., Paduch, M., Medovoy, D., Singharoy, A., McGreevy, R., Villalba-Galea, C.A., Hulse, R.E., Roux, B., Schulten, K., et al. Structural mechanism of voltage-dependent gating in an isolated voltage-sensing domain. *Nat. Struct. Mol. Biol*. **21**: 244–252 (2014).

McCoy, A.J., Grosse-Kunstleve, R.W., Adams, P.D., Winn, M.D., Storoni, L.C., and Read, R.J. Phaser crystallographic software. *J. Appl. Cryst*. **40**: 658–674 (2007).

Muroi Y, Arcisio-Miranda M, Chowdhury S, Chanda B. Molecular determinants of coupling between the domain III voltage sensor and pore of a sodium channel. *Nat Struct Mol Biol*. **17**(2): 101-112 (2010).

Murshudov, G.N., Skuba´ k, P., Lebedev, A.A., Pannu, N.S., Steiner, R.A., Nich- olls, R.A., Winn, M.D., Long, F., and Vagin, A.A. REFMAC5 for the refinement of macromolecular crystal structures. *Acta Crystallogr. D Biol. Crystallogr*. **67**: 355–367 (2011).

Noda M, Hiyama TY. The Na(x) Channel: What It Is and What It Does. *Neuroscientist*. **21**(4): 399-412 (2015).

Otwinowski, Z., and Minor, W. Processing of X-ray diffraction data collected in oscillation mode. *Methods Enzymol*. **276**: 307–326 (1997).

Pan X, Li Z, Zhou Q, et al. Structure of the human voltage-gated sodium channel $Na_v1.4$ in complex with β1. *Science*. **362** (2018).

Payandeh, J., Scheuer, T., Zheng, N., and Catterall, W.A. The crystal structure of a voltage-gated sodium channel. *Nature.* **475**: 353–358 (2011).

Pless SA, Elstone FD, Niciforovic AP, et al. Asymmetric functional contributions of acidic and aromatic side chains in sodium channel voltage-sensor domains. *J Gen Physiol*. **143**(5): 645-656 (2014).

Rush AM, Cummins TR, Waxman SG. Multiple sodium channels and their roles in electrogenesis within dorsal root ganglion neurons. *J Physiol*. **579**(Pt 1): 1-14 (2007).

Shen H, Liu D, Wu K, Lei J, Yan N. Structures of human $Na_v1.7$ channel in complex with auxiliary subunits and animal toxins. *Science*. **363**(6433): 1303-1308 (2019).

Toledo-Aral JJ, Moss BL, He ZJ, et al. Identification of PN1, a predominant voltage-dependent sodium channel expressed principally in peripheral neurons. *Proc Natl Acad Sci U S A*. **94**(4): 1527-1532 (1997).

Winn, M.D., Ballard, C.C., Cowtan, K.D., Dodson, E.J., Emsley, P., Evans, P.R., Keegan, R.M., Krissinel, E.B., Leslie, A.G., McCoy, A., et al. Over- view of the CCP4 suite and current developments. *Acta Crystallogr. D Biol. Crystallogr.* **67**: 235–242 (2011).

Wisedchaisri G, Tonggu L, McCord E, et al. Resting-state structure and gating mechanism of a voltage-gated sodium channel. *Cell*. **178**(4): 993-1003 (2019).

Yang Y, Wang Y, Li S, et al. Mutations in SCN9A, encoding a sodium channel alpha subunit, in patients with primary erythermalgia. *J Med Genet*. **41**(3): 171-174 (2004).

Yang Y, Mis MA, Estacion M, Dib-Hajj SD, Waxman SG. $Na_V1.7$ as a pharmacogenomic target for pain: moving toward precision medicine. *Trends Pharmacol Sci*. **39**(3): 258-275 (2008).